Talanta 246 (2022) 123473

Contents lists available at ScienceDirect

Talanta

journal homepage: www.elsevier.com/locate/talanta

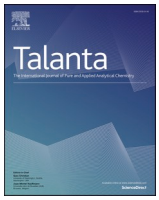

Potentiometric detection of creatinine in the presence of nicotine: Molecular recognition, sensing and quantification through multivariate regression

Alessandro Corba [a,d], Andrés F. Sierra [a,b], Pascal Blondeau [a], Barbara Giussani [d], Jordi Riu [a], Pablo Ballester [b,c], Francisco J. Andrade [a,*]

[a] Departament de Química Analítica i Química Orgànica. Universitat Rovira i Virgili (URV), C/ Marcel·lí Domingo 1, 43007, Tarragona, Spain
[b] Institute of Chemical Research of Catalonia (ICIQ). The Barcelona Institute of Science and Technology, Av. Països Catalans, 16, 43007, Tarragona, Spain
[c] Catalan Institution for Research and Advanced Studies (ICREA), Pg. Lluís Companys 23, 08010, Barcelona, Spain
[d] Dipartimento di Scienza e Alta Tecnologia, Università degli Studi dell'Insubria, Via Valleggio, 9, 22100, Como, Italy

A B S T R A C T

Systematic errors in the calix [4] pyrrole-based potentiometric detection of creatinine have been observed in heavy smokers. This work further characterizes the interactions between the nicotinium cation and the cavitand as well as the resulting interference produced during the potentiometric detection. It is found that the nicotinium cation binds the electronic rich aromatic cavity defined by the pyrrole rings of the receptor's cone conformation with an estimated binding constant higher than 10^{-4} M^{-1} in methylene chloride. On the other hand, the creatininium cation is preferentially included in the hydrophobic aromatic cavity of the ionophore by establishing hydrogen bond interactions with the pyrrole NHs groups. Potentiometric calibrations confirmed the detection of the nicotinium cation at neutral and acidic pH, respectively. Due to the lower pka of creatinine, a methodology to quantify creatinine in presence of nicotine by using an array of three sensors at two pH values is proposed. A partial least squares regression was performed and reported recoveries of 103% with a standard deviation of 20%. The improved determination of creatinine was therefore discussed. This approach represents a step forward in the development of effective approaches to improve the measurement of creatinine in decentralized settings.

1. Introduction

Monitoring chronic conditions is becoming a growing challenge in healthcare, with significant implications in analytical chemistry. Indeed, as the use of information and communication platforms is driving the evolution towards remote care approaches, there is a growing pressure to transform conventional lab-based instruments into point of care devices. An example that pioneered and anticipated this trend is the long quest to improve the management of diabetes, which resulted in the development of the glucometer. Initially conceived for clinical settings, this device was then adapted for home use and its success has fueled the search for similar solutions in other areas. From an analytical perspective, the challenge is to develop tools for monitoring biomarkers that can simultaneously meet analytical, as well as mass-market standards. Simple, robust, and affordable approaches are increasingly required.

Creatinine is -together with glucose-one of the top biomarkers of interest. Creatinine is continuously produced by the muscles and transported by the blood stream to the kidneys, where it must be excreted through the glomerular filtration process. For this reason, creatinine is one of the key biomarkers for monitoring kidney conditions, in particular for detecting and diagnosing chronic kidney disease (CKD) [1]. CKD is a silent condition that progress unnoticed until well advanced, and for that reason is in the top 10 chronic conditions in adults worldwide [2]. Strongly associated to other pathologies, such as diabetes and cardiovascular disease, stage of progression of CKD is defined by the creatinine blood levels. Surprisingly, despite of being such a fundamental parameter, current analytical methods for performing this analysis are complex, outdated, and prone to error.

In the clinical laboratory the determination of creatinine is routinely performed with methods based on the Jaffé reaction, an approach that was reported almost 150 years ago [3]. Despite of its widespread use, this is a complex kinetic-based approach that uses delicate reagents and is prone to interferences that tend to produce inaccurate results. Therefore, it can hardly assume a point of care format. Several alternatives have been reported in the scientific literature [4,5] and there are also some commercial portable devices specific for the determination of

* Corresponding author. Departament de Química Analítica i Química Orgànica. Universitat Rovira i Virgili (URV), C/ Marcel·lí Domingo 1, 43007, Tarragona, Spain.
E-mail address: franciscojavier.andrade@urv.cat (F.J. Andrade).

https://doi.org/10.1016/j.talanta.2022.123473
Received 7 March 2022; Received in revised form 7 April 2022; Accepted 8 April 2022
Available online 13 April 2022
0039-9140/© 2022 The Authors. Published by Elsevier B.V. This is an open access article under the CC BY license (http://creativecommons.org/licenses/by/4.0/).

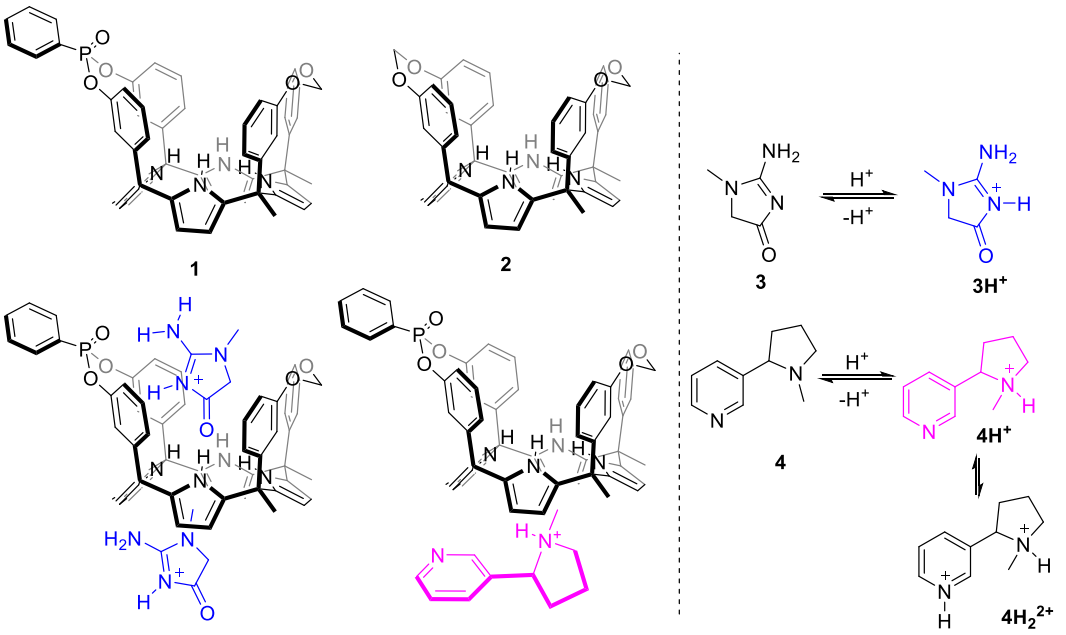

Scheme 1. Tetra-aryl-substituted, monophosphonate-bridged calix [4]pyrrole (ionophore **1**); reference receptor (ionophore **2**); line-drawing structures of creatinine (**3**) its protonated form, the creatininium cation (**3**H^+) featuring a pka = 4.8; nicotine (**4**) and its protonated form, the nicotinium cation (**4**H^+) having a pka = 7.9 and the nicotinium dication (**4**H_2^{2+}) with pka = 3.2. Line-drawing structures of the putative 2:1 complex of the creatininium cation with ionophore **1** and the 1:1 complex of the nicotininium cation with the same ionophore.

creatinine. However, most of them are based on three enzyme cascade approaches that require careful control of the reaction conditions [6]. All in all, as most tools are complex and only suited for professional use, there is a growing need for simple, robust and affordable tools for the determination of creatinine in clinical samples.

During the last few years we have reported a novel ion-selective potentiometric approach for the determination of creatinine in blood and urine [7]. Potentiometry is an ideal technique for building point of care devices, since it combines robustness, simplicity of operation and instrumentation and low cost. One of its main limitations is the reduced number of substances that can be detected. To overcome this issue, we have developed a novel ionophore with a high selectivity for creatinine. First, an aryl-substituted, monophosphonate-bridged calix [4]pyrrole phosphonate cavitand **1** (Scheme 1, ionophore **1**) was designed and synthesized to demonstrate efficient binding with the creatinine and the creatininium cation in solution. In a previous work, we have shown that the affinity of the ionophore for creatinine strongly depends on the aryl-phosponate bridge. Therefore, a molecule without this bridging group was used as reference (ionophore 2). Second, ionophore **1** was incorporated into a suitable polymeric matrix allowing simple, selective, fast and enzyme-free potentiometric detection of creatinine. The method, which only requires adjusting the pH of the solution to convert creatinine into the charged creatininium cation, was validated through the accurate direct detection of creatinine in urine samples [8]. However, like any other potentiometric approach, the sensing method presents two major limitations: a) the unspecific (bio)fouling produced by large biomolecules and b) the more specific interferences due to the affinity of the ionophore with small organic and inorganic species. In urine -where the levels of creatinine are higher-the first issue has been successfully overcome by sample dilution. Nevertheless, some errors resulting in abnormally high values have raised questions regarding specific interferences linked to the selectivity of the ionophore 1.

The selectivity of ionophore **1** towards common cations (K^+, Na^+ etc …) is high enough to allow the direct determination of creatinine biological matrices [7,8]. However, screening of data revealed some association between abnormally high values of creatinine and smoking habits. Considering that the cationic form of nicotine (4H^+), produced at the pH used in the determination of creatinine,is a lipophilic molecule, we surmised that the putative existence of an interaction between the nicotinium cation and the ionophore **1** could cause the observed interferences during the detection of creatinine. Calix [4]pyrrole receptors can function as heteroditopic receptors. They bind electron rich species and anions by including them in its deep and polar aromatic cavity by establishing complementary hydrogen bonding interactions, i.e. recognition of creatinine. Moreover, calix [4]pyrrole receptors can also bind cations in the shallow and electron-rich aromatic cavity, opposed to bound electron-rich species, that is defined by the pyrrole rings in cone conformation (i.e. cation-pi interactions) [7]. Previously, we described that the interaction between the creatininium cation and ionophore **1** produced 1.1 and 2:1 complexes. In the 2:1 complex, one creatininium cation is included in the polar cavity of the ionophore and a second cation located its methyl group in the opposed electron-rich cavity (Scheme 1). The oxygen atom of the included creatininium cation was engage in four convergent hydrogen bonds with the pyrrole NHs at the closed end of the cavity. In turn, the methyl group of a second creatininium cation was inserted in the opposed electron-rich cavity of the bound calix [4]pyrrole establishing cation-pi interactions with the pyrrole rings. In the case of the potentiometric detection of creatininium, we hypothesized that the formation of the inclusion 1:1 host-guest complex was the main responsible of the sensing. Nevertheless, for the nicotinium cation, and related metabolites, the formation of a 1:1 complex exclusively located the methyl group in the electron rich aromatic cavity defined by the pyrrole rings of the calix [4]pyrrole receptor in cone conformation (Scheme 1) [9].

One of the major limitations of the implementation of ISEs is indeed the demanding selectivity requirements. The K^+ ISE, for instance, suffers from the interference of ammonium due to comparable size and enhanced lipophilic character of the later [10]. For anions, this issue is even more pronounced due the strong hydration enthalpy [11] and for instance the potentiometric recognition of highly hydrophilic anions such as sulfate and phosphate still remains challenging [12]. Overcoming interferences through sample pretreatment (e.g., precipitation of salts with pH control [13], etc.) is possible, but limited to laboratory and complex to perform in real samples. Alternatively, designing sensor

Table 1
Analytical figures of merit of sensor 1 and blank for nicotine in acidic (pH 3.8) and neutral buffer (pH 7.4).

	Sensor 1		Blank	
pH	3.8	7.4	3.8	7.4
Sensitivity (mV/decade)	57.5 ± 2.1	52.7 ± 0.5	51.8 ± 0.9	51.4 ± 1.5
Linear range (Log)	−6 to −2	−5 to −2	−5 to −2	−5 to −2
Log (LOD)	−6.53 ± 0.06	−5.11 ± 0.01	−5.42 ± 0.02	−5.02 ± 0.01

arrays that can increase the channels of information is emerging as an attractive approach to improve the detection of the primary analyte and even expand to multianalyte detection [14].

In this work, we present first the evidence that confirms the specific interference on the potentiometric detection of creatinine produced by the nicotininium cation. It is shown that an electrode incorporating ionophore **1** presents an enhanced detection to the nicotininium cation in acidic and neutral media. 1D and 2D NMR spectroscopy studies are used to probe the interaction between the ionophore **1** and the nicotinium cation in solution. Thereafter, a sensor array incorporating ISEs of ionophore **1** and **2** (lacking the phosphonate group inwardly directed with respect to the cavity) and an additional ISE lacking of any ionophore (labelled as blank sensor) was designed and characterized. Based on these results, we propose an unprecedented methodology to determine creatinine in presence of nicotine by using an array of three potentiometric sensors measuring at two different pHs. Indeed, taking advantage of the low pKa value of creatinine (4.8) compared to the first one of nicotine (3.2 and 7.9), samples were measured in both acidic and neutral conditions [15]. Multivariate analysis allows thus generating a model for the detection of creatinine in presence of nicotine with good recoveries. These results encourage the development of potentiometric sensing arrays that can be successfully applied to monitoring chronic conditions.

2. Experimental

2.1. Reagents

Potassium tetrakis[3,5-bis-(trifluoromethyl)phenyl] borate (KTFPB), *o*-nitrophenyl octyl ether (*o*-NPOE) >99%, high molecular weight polyvinyl chloride (PVC), anhydrous tetrahydrofuran (THF) > 99.9%, magnesium acetate tetrahydrate ($Mg(Ac)_2{\cdot}4H_2O$) > 99%, sodium tetraborate ($Na_2B_4O_7$) 99%, sodium acetate (NaAc) > 99%, sodium phosphate monobasic (NaH_2PO_4) >99%, sodium hydrogen phosphate (Na_2HPO_4), potassium di-hydrogen phosphate (KH_2PO_4), lithium di-hydrogen phosphate (LiH_2PO_4), analytical grade chloride salts of sodium (NaCl), potassium (KCl), creatinine anhydrous >98%, (−)-nicotine >99%, hydrochloric acid 37% (HCl), hydrochloric acid (4 M in dioxane), sodium hydroxide (NaOH), (TRIS-HCl) tris(hydroxymethyl) aminomethane hydrochloride (TRIS-HCl), 3-(N-morpholino)propanesulfonic acid (MOPS), 2-(N-morpholino)ethanesulfonic acid (MES), Sodium tetrakis [3,5-bis(trifluoromethyl)phenyl]borate ($NaBArF_4$) and ethyl ether were all purchased from Sigma-Aldrich (Spain). Acetic Acid (96% purity) was purchased from Riedel-de Häen (Honeywell International Inc., Germany).

All solutions were prepared using doubly deionized water (18.1 MΩ cm^{-1} resistance) produced by a Milli-Q water system (Millipore Corporation, Bedford, MA). Buffer solutions were prepared as mentioned elsewhere [8]. Briefly: 50 mM acetic acid/magnesium acetate (HAc/Mg $(Ac)_2$) pH 3.8; and 50 mM phosphate buffer (PB with potassium or lithium as counteraction) pH 7.4 as well as MOPs and TRIS-HCl pH 7.4.

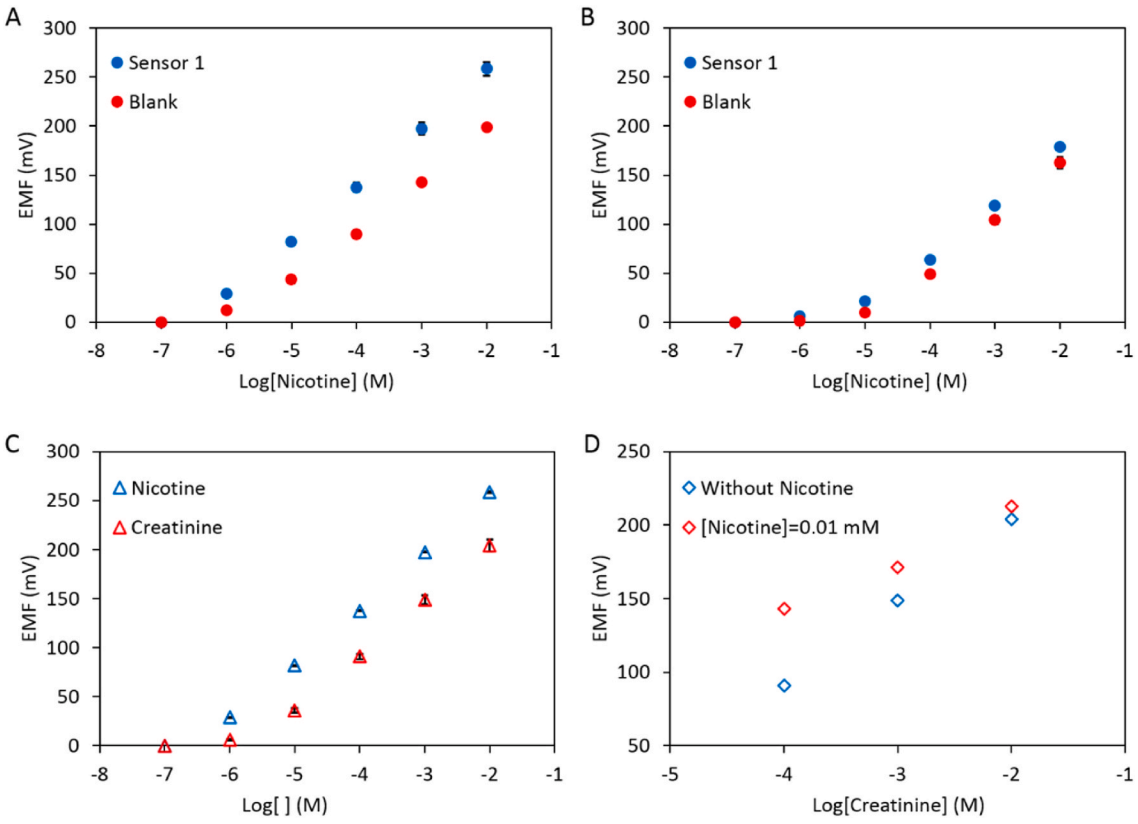

Fig. 1. Calibration curve of nicotine with sensor 1 and blank at A) pH 3.8 and B) pH 7.4; C) Comparison of the independent response of sensor 1 to creatinine and nicotine at pH 3.8; D) Calibration of creatinine with sensor 1 (at pH 3.8) in the absence (blue dots) and in the presence of 0.01 mM nicotine. Error bars correspond the measurement of three different sensors (N = 3). (For interpretation of the references to colour in this figure legend, the reader is referred to the Web version of this article.)

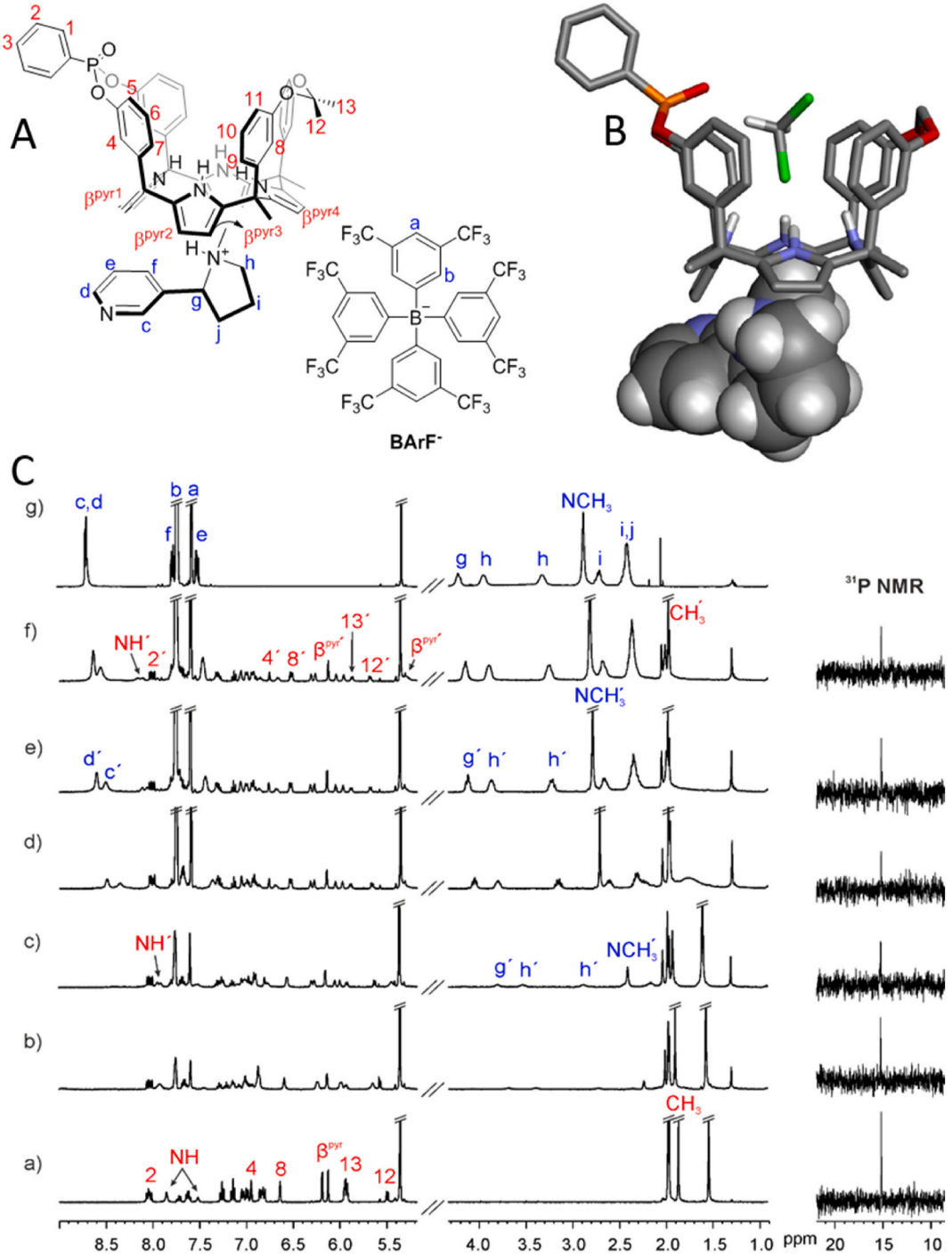

Fig. 2. A) Line-drawing structure of the 1:1 complex of ionophore **1** with $BArF_4$ salt of nicotininium cation $\mathbf{4H}^+$, B) Front view of the energy minimized structure of the complex (BP86-D3/def2-SVP). C) Selected regions of the ^{1}H NMR and ^{31}P NMR spectra registered during the titration of a millimolar solution of ionophore **1** (a) with incremental amounts of the BAr^F_4 salt of nicotinium cation in CD_2Cl_2 solution, b) 0.5 equiv, c) 1.0 equiv, d) 3.0 equiv, e) 5.0 equiv, f) 9.0 equiv, g) Free $BArF_4$ salt of nicotinium cation.

Preparation of the ion-selective membrane is described elsewhere [7]. Briefly, the membrane of sensor 1, 2 and blank were prepared using a 1:2 wt ratio of polymer (PVC) and plasticizer (*o*-NPOE) respectively (see Table 1 for complete composition). This mixture was vigorously shaken for 30 min in an ultrasonic bath (37Hz, 100% power, FB11205, Fisherbrand®) until complete dissolution of all the components. Afterwards, 50 μL of the mixture were deposited by drop casting onto a glassy carbon electrode and allowed to dry for a minimum of 2 h. The selectivity coefficient was calculated with the separated solution method (SSM) [16] and the required selectivity coefficients with the maximally tolerable errors based on our previous work [17].

2.2. Instrumentation

Electromotive force (EMF) was measured with a high input impedance device (10^{15} Ω EMF16 multichannel data acquisition, Lawson Laboratories, Inc. Malvern, USA) at room temperature (22 °C) in a well-stirred solution. A double junction 3 M Ag/AgCl/KCl reference electrode

(type 6.0726.100, Methrom AG) containing a 1 M LiAcO electrode bridge was used.

2.3. Synthesis

The synthesis of $[BArF_4]^-[\mathbf{4}H]^+$ involved two reaction steps starting for the precipitation of the nicotine hydrochloride, $[Cl]^-[\mathbf{4}H]^+$, from a nicotine ether solution by addition of hydrochloric acid (in dioxane). The pure salt was isolated quantitatively after a Schlenk-frit filtration under argon atmosphere. Finally, the anion exchange was achieved by reacting $[Cl]^-[\mathbf{4}H]^+$ with $NaBArF_4$ in water at 98 °C. The reaction produce a precipitated which was filtered and washed with water yielded pure $[BArF_4]^-[\mathbf{4}H]^+$ in 75% (see experimental details in SI for full characterization).

2.4. Multivariate model for the prediction of creatinine

PLS Toolbox 8.8.1 (Eigenvector Inc, Manson, WA, USA) for MATLAB 2020a (Mathworks Inc., Natick, MA, USA) was used for data analysis. Partial least squares (PLS) regression was used for quantitative analysis. Data from the six recorded EMF values (blank, ionophore 1 and ionophore 2 at pH 3.8, and blank, ionophore 1 and ionophore 2 at pH 7.4) were used to build the **X** matrix. The concentration of creatinine in the samples (expressed as logarithm of concentration) was used for the **y** matrix. All the data were mean-centered before the construction of the PLS model. No other pre-treatments were applied in the construction of the models. The Venetian blinds method (with 14 data splits and three samples per blind) was used for the cross-validation. Root mean square error of cross-validation (RMSECV) was chosen as the figure of merit to check the usefulness of the model.

3. Results and discussion

3.1. Potentiometric detection of nicotine

The creatininium cation has a pKa value of 4.8, which means that at pH 3.8 it will be the predominant form of creatinine. For this reason, this pH was originally chosen as the optimum value for the potentiometric detection of creatinine [8]. At pH 7.4 only the neutral form of creatinine is found. Nicotine, on the other hand, has divalent and monovalent cations, with pKa values of 3.2 and 7.9 respectively. Thus, while at both pH values the monovalent is the predominant species, at pH 3.8 there is a significant fraction of both, di- and mono-valent cations, while at pH 7.4 (PBS buffer) a significant fraction of the monovalent cation and neutral species exist.

Potentiometric sensors with and without the incorporation of ionophore **1** were prepared and labelled as sensor 1 and blank, respectively (see Table S1). Fig. 1 (A and B) compares the calibration curve obtained for sensor 1 and blank at both pH (3.8 and 7.4). The results show that the presence of the ionophore **1** (sensor 1) enhances the detection of nicotine, thus confirming that interactions between the ionophore 1 and the nicotinium cation occur. The higher potentiometric response obtained at acidic pH might be due to the lower level of interfering cations present in the acetic buffer (Mg^{2+}) compared to PB buffer (Na^+/K^+). Alternative buffer compositions were also tested as an attempt to improve the detection of nicotinium at pH 7.4. The use of 50 mM MOPs and TRIS-HCl buffers yielded a higher total potentiometric response for both sensor 1 and blank. Unfortunately, in these ammonium-based buffers the response of the blank was higher than that of sensor 1. Most likely and as explained above, this is due to unspecific interactions between the buffer components and the ionophore 1 [9]. For this reason, the rest of the experiments in neutral media were conducted in PB pH 7.4. The results of the calibration for nicotine using sensor 1 and blank are shown in Table 1, where the sensitivity, linear range and limits of detection (LOD) are compared. It is worth mentioning that at pH 3.8 sensor 1 produces a Nernstian response (57.5 ± 2.1 mV/dec) for nicotine down to the single μM range. This value is one order of magnitude lower than for the blank sensor (Table 1). In general, reports on potentiometric detection of nicotine are scarce, with analytical performance poorer than the herein reported example [18–20].

Once the detection of nicotine with sensor 1 has been demonstrated, a comparison of the separate detection of both analytes, nicotine and creatinine, was conducted. Fig. 1C compares the independent detection of nicotine and creatinine at pH 3.8 using sensor 1. These results confirm that nicotine may produce a significant interference on the detection of creatinine at the working pH. A selectivity coefficient calculated with the separate solution method yields a value of log $K_{Creatinine,\ Nicotine} = +1.07 \pm 0.1$. To put things in perspective, the levels of error (from 1 to 100%, Table S2) for different values of selectivity coefficients were estimated, considering the clinical range for creatinine and nicotine in urine are between 3 and 25 mM [21] and 0.006–0.04 mM [22], respectively.

Empirical evidence of this interference can be seen in Fig. 1D, where the effects of performing a calibration of creatinine with sensor 1 in a background of nicotine 0.01 mM are shown. Evidently, as the ratio nicotine/creatinine increases the interference becomes more serious. Fig. 1D shows that even for a ratio 1:100 (1 mM creatinine in a 0.01 mM nicotine) the interference is significant.

3.2. Supramolecular interactions of the nicotine-ionophore system

The $BArF_4$ salt of nicotine was synthetized in order to probe the non-covalent interactions between the ionophore **1** and the nicotininium cation $\mathbf{4}H^+$. We selected tetrakis(3,5-bis(trifluoromethyl)phenyl)borate ($[BArF_4]^-$) as solubilizing and non-competitive counterion for the nicotinium cation in non-polar organic solvents.

We isolated the $[BArF_4]^-$ salt of $\mathbf{4}H^+$ in 75% yield. The salt was characterized by a set of high-resolution spectra and X-ray crystallography (Figures S1-4). We performed titrations experiments of **1** with $[BArF_4]^-[\mathbf{4}H]^+$ in CD_2Cl_2 solution using ^1H and ^{31}P NMR spectroscopy. The ^1H NMR spectrum of a millimolar solution of receptor **1** in CD_2Cl_2 showed sharp and well-resolved proton signals that agree with *Cs* symmetry (Fig. 2C, left side). Additionally, the ^{31}P NMR spectrum of **1** showed a single phosphorous signal (Fig. 2C, right side). The incremental addition of the $BArF_4$ salt of nicotine induced chemical shift changes to the proton signals of the ionophore **1**.

Remarkably, the ^{31}P NMR spectra acquired during the titration evidenced that the phosphorous signal of receptor **1** was not affected by the incremental addition of the $BArF_4$ salt of nicotine. (Fig. 2C, right side). This observation suggests that the P═O group is not involved in the binding with the nicotinium cation. We performed a detailed analysis of three spectral regions of NMR spectra acquired during the titration experiments (Figures S5-8). We observed that in response to the incremental addition of the $BArF_4$ salt of the nicotinium cation the pyrrole NHs of ionophore **1** moved slightly downfield ($\Delta\delta = +$ 0.6–0.3 ppm). Other proton signals of **1** also experienced reduced chemical shift changes. After the addition of more than 1 equiv of $[BArF_4]^-[\mathbf{4}H]^+$, the signals of the ionophore **1** did not experience noticeable changes. Taken together, the obtained results indicated that the binding of 1 with $[BArF_4]^-[\mathbf{4}H]^+$ produced a complex with 1:1 stoichiometry for which we can estimate a binding constant larger than 10^4 M^{-1}. The binding equilibrium between free and bound counterparts experiences exchange dynamics that were fast on the chemical shift timescale. We also observed that the increase in the concentration of the nicotinium cation produced a significant downfield shift to its methyl group signal (singlet). This observation indicated that the bound nicotinium cation placed its methyl group in the shallow and electron rich cavity of **1**. In this location, the methyl groups experienced the shielding effect of the four pyrrole rings. Owing to the fast chemical exchange that exist between the free and bound cation, after the addition of 1 equiv, the increase in concentration provokes the presence of incremental amounts of the free counterpart, thus explaining the observed downfield towards

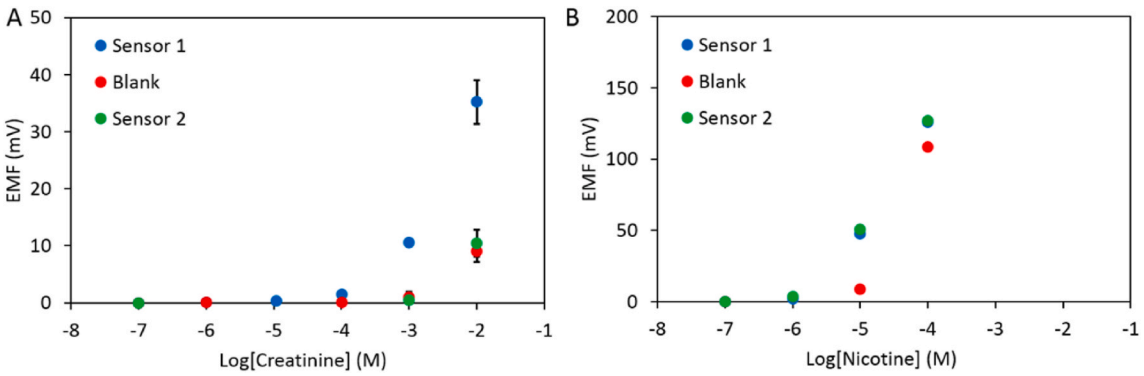

Fig. 3. Potentiometric response of a creatinine (A) and nicotine (B) at pH 7.4 for sensor 1, blank, and sensor 2.

the chemical shift value of the free cation (Figures S9-11). We further characterized the 1:1 complex using a dichloromethane solution containing an equimolar mixture of **1** and the $BArF_4$ salt of nicotinium. The NOESY experiment of the mixture showed the existence of cross-peaks due to close-proximity in space between the methyl group of the nicotinium cation and the β-pyrrole protons of 1. This result fully supported

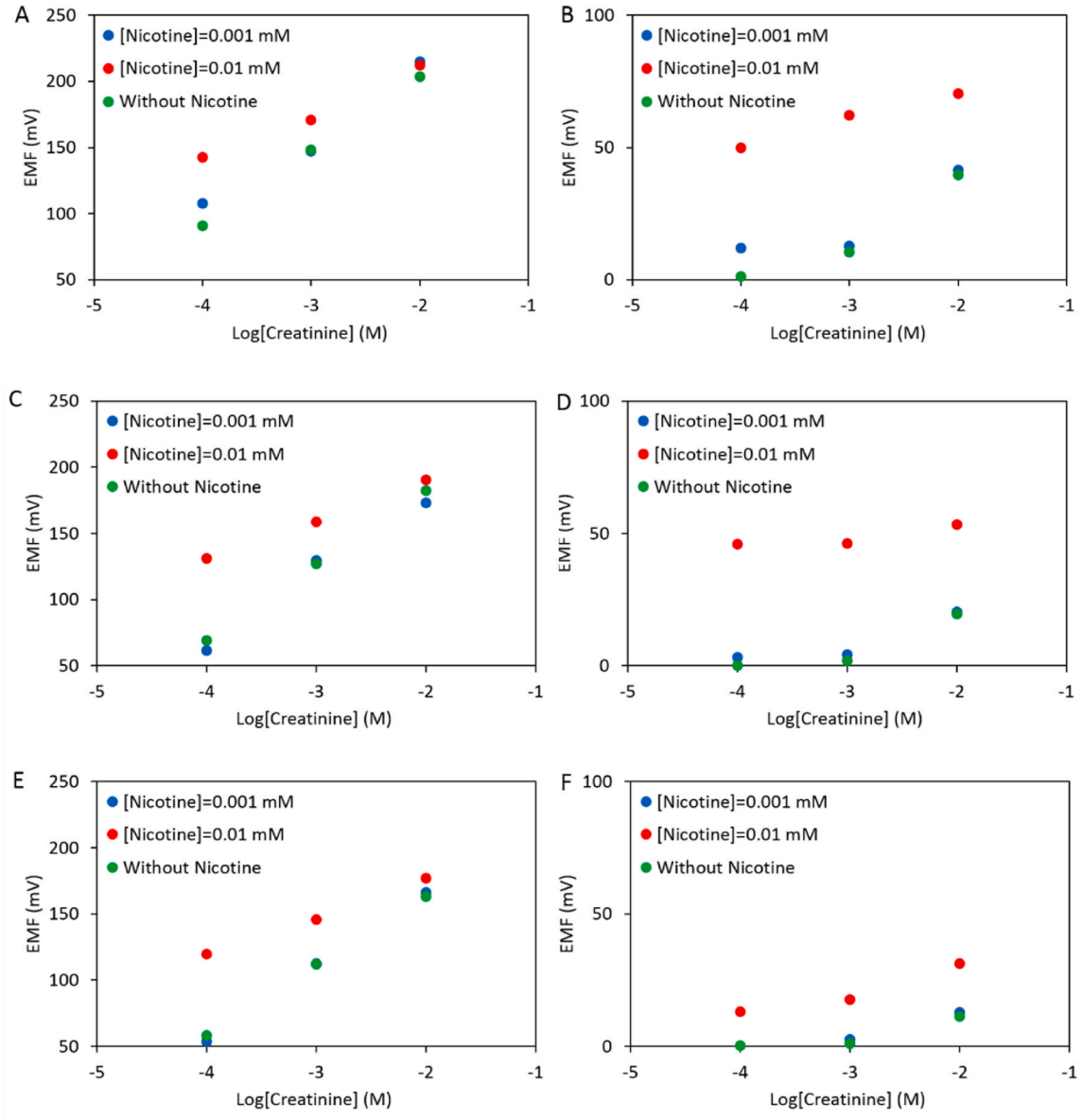

Fig. 4. Potentiometric response for creatinine at pH 3.8 (A, C, E) and pH 7.4 (B, D, F) for sensor 1 (A, B), sensor 2 (C, D) and blank, (E, F).

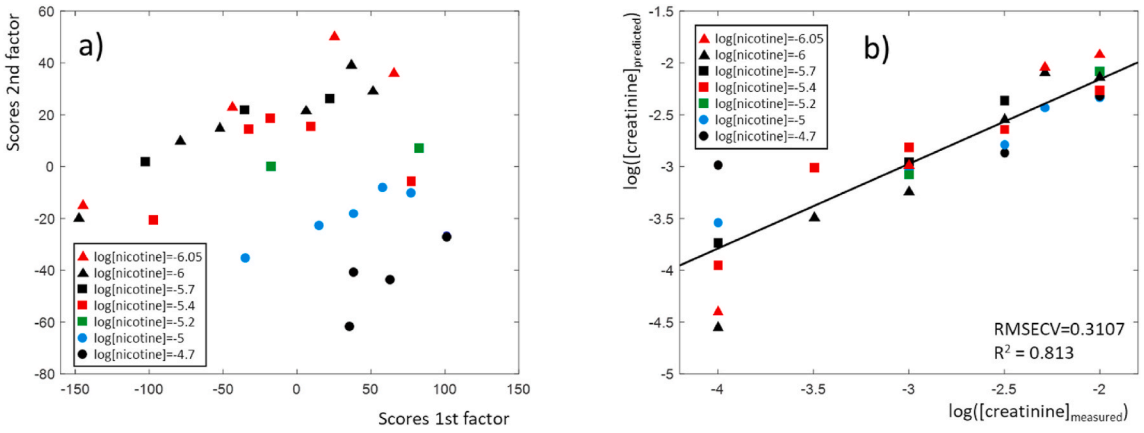

Fig. 5. a) Scores plot of the PCA model containing all the samples. Two factors explained the 87.15% of the original information in the y-variable. b) Regression line between the measured concentrations of creatinine and the predicted concentrations of creatinine with the PLS model.

that in the 1:1 complex quantitatively formed in solution, the methyl group of the protonated nicotine cation was located in the shallow and electron rich cavity of the receptor's cone conformation (Figures S12-19, Table S3). Most likely, the 1:1 cationic complex is fully dissociated in solution owing to the reduced coordination properties of the $[BArF_4]^-$ anion. It is worthy to note, for comparison purposes, that the reported binding constants of the 1:1 and 2:1 complexes of **1** with the creatininium cations are of the same order of magnitude ($\sim 10^4$ M^{-1}) under similar conditions [7].

Fig. 2B shows a side view of the energy-minimized structures of the putative 1:1 complex of ionophore **1** with protonated nicotine **4**H^+. The $[BArF_4]^-$ counter anion was removed to simplify the calculation and because in solution we assumed that the complex is significantly dissociated. We included one methylene chloride molecule bound inside the cavity of the ionophore **1** in order to stabilize the cone conformation. The energy-minimized structure of the complex was performed at the BP86-D3/def2-SVP level of theory as implemented in TURBOMOLE version 7 [23–26].

3.3. *Potentiometric detection of creatinine in presence of nicotine*

All the evidence confirms that nicotine can have a powerful interfering effect in the potentiometric determination of creatinine, due to the strong interactions between the nicotinium cation and the ionophore **1**. Therefore, an approach to overcome this issue, allowing the accurate detection of creatinine in the presence of nicotine, has been elaborated. The proposed strategy follows three main lines. First, using the pH as discriminating variable, since it has been already shown that for sensor 1 and the blank the response of creatinine and nicotine as function of pH is different. Second, introducing an additional sensing device (sensor 2) to increase the power of discrimination between the two species. Third, using multivariate statistical tools to extract the information and improve the determination.

The additional channel, sensor 2, was built using ionophore 2. The details on the use of this ionophore for the detection of creatinine can be seen elsewhere [7]. In essence, sensor 1 provides information of both, nicotine and creatinine. For sensor 2, on the other hand, the lack of the bridging-phosphonate group reduces its response to creatinine. However, because of the different type of complexes formed in the interaction of the two cations with the ionophores, the lack of the bridging-phosphonate is not expected to affect significantly the potentiometric detection of the nicotinium cation. In fact, a preliminary screening (data not shown) reveals that this assumption is correct, and sensor 2 responds to nicotine at both pH. Finally, the blank sensor provides a nonspecific response which is linked to the lipophilicity and ion-exchange capacity of the membrane. Therefore, a sensing array containing sensor 1, sensor 2 and the blank sensor was built and tested within the clinical range of interest, which for creatinine is up to 10 mM and for nicotine up to 0.1 mM, in solutions of pH 3.8 and 7.4. First, individual analyte responses were evaluated and then mixed solutions were considered.

The results show that at pH 7.4 (Fig. 3A), the response for creatinine is better for sensor 1 than for sensor 2 (which is similar to the blank). This is due to the additional hydrogen bonding interaction that the bound creatininium cation can establish with the bridging phosphonate group present at the upper rim of ionophore 1, compared to ionophore 2 that lacks of the bridging phosphonate. Evidently, the response of creatinine is limited due to the minimal fraction of the analyte present as creatininium cation (capable of producing the potentiometric response) at this pH. In the case of nicotine at pH 7.4 (Fig. 3B), both sensor, 1 and 2 show similar response, which is significantly larger than the response of creatinine (in part due to the higher fraction of nicotinium cation) and also enhanced compared to blank. This confirms our previous assumption: ionophores **1** and **2** should provide similar potentiometric responses to nicotine because the non-covalent interactions (cation-π) established between the analyte and the ionophores involve their almost identical shallow and electron-rich cavities.

In order to optimize the use of the sensor array, testing solutions of creatinine in different background of nicotine were tested. Fig. 4 shows the calibrations of creatinine at both pHs for sensor 1, sensor 2 and the blank sensor. While at nicotine levels of 0.001 mM the contribution is very low (negligible for sensor 2 and blank), when nicotine is at a concentration of 0.01 mM its contribution to the potentiometric response is significant, at both pH values. In the presence of nicotine at these levels of concentration (typical for smokers) the relationship between the potentiometric response and the concentration of creatinine is blurred and cannot be established with a univariate calibration strategy. Since both substances contribute to the potentiometric response, but their contributions are pH-dependent, a multivariate calibration approach seems more appropriate.

PLS was used to correlate the concentration of creatinine in the samples (expressed as logarithm of concentration) with the six recorded EMF values (sensor 1 and 2, blank at both pHs 3.8 and 7.4). Two factors explained 87.1% of the original information in the y-variable (concentration of creatinine), with a root mean square error of cross-validation (RMSECV) of 0.3107. RMSECV is given in logarithmic concentration units and indicates the averaged errors in quantification of the target analytes with the derived models. Despite RMSECV has its limitations when applied to a range of logarithmic concentrations since it is a point estimation, it is a widely used figure of merit in model comparison [27].

The scores plot (Fig. 5A) shows that the samples with higher concentration of nicotine ($10^{-4.7}$ and 10^{-5} M) appear in different groups in

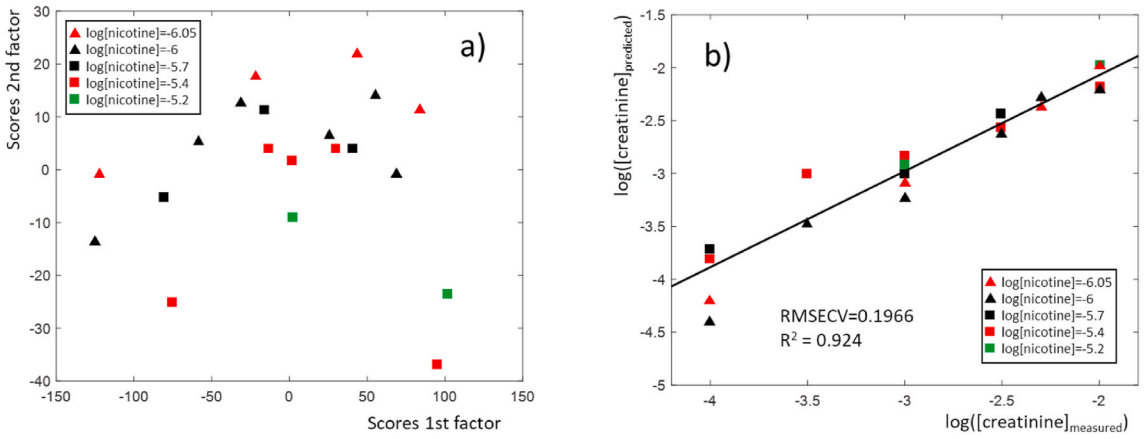

Fig. 6. a) Scores plot of the PCA model removing the samples containing high concentration of nicotine. Two factors of the PLS model explained 94.64% of the original information in the y-variable. b) Regression line between the measured concentrations of creatinine and the predicted concentrations of creatinine with the PLS model.

the lower-right part of the graph, while the rest of samples are uniformly mixed. The score plot confirms the importance of the nicotine values in building a calibration model for the prediction of creatinine. The plot of predicted versus measured concentrations of creatinine (Fig. 5B) shows that the predicted values at the lower concentrations have a very high variability. In particular, higher errors in the prediction of concentrations of creatinine are found for higher concentrations of nicotine.

To check this hypothesis, samples containing high concentration of nicotine ($10^{-4.7}$ and 10^{-5} M) were removed and the PLS model was rebuilt. In this case, two factors of the PLS model explained 94.64% of the original information in the y-variable, with an improved RMSECV of 0.1966. The scores plot shows in this case no dependence from the concentration of nicotine (Fig. 6A). In Fig. 6B the predicted versus measured concentrations of creatinine plot shows that the variability of the predictions is not related to the nicotine content in the samples.

This model was then externally validated with the test-set method, finding the recovery values for the predicted samples in the test set. The set of samples were divided into a training set (75% of the samples randomly selected at each concentration level were used to build the model) and a test set (25% of the samples randomly selected at each concentration level were used to validate the model), ensuring therefore that all the concentration levels were included in both the training and test sets. The average predicted recoveries ($[creatinine]_{real}/[creatinine]_{predicted}$ 100) of the test set was 97% with a standard deviation of 26%.

To mimic physiological concentrations of creatinine and nicotine in urine, samples with concentrations of creatinine below 10^{-3} M were removed. The resulting PLS model improved the previous results and two factors explained 95.26% of the original information in the y-variable, with a RMSECV of 0.1255. In order to perform an external validation of the model, the set of samples was divided again into a training set (≈70% of the samples randomly selected at each concentration level were used to build the model) and a test set (≈30% of the samples randomly selected at each concentration level were used to build the model), ensuring again that all the concentration levels were included in both the training and test sets. The average predicted recoveries of the test set was 103% with a standard deviation of 20%.

4. Conclusions

This work represents a step forward in the development of robust and simple analytical tools that can be used in the evaluation of chronic conditions. First, it has been shown that nicotine is a significant specific interference in the potentiometric determination of creatinine with sensor 1, due to the strong interactions established between the ionophore **1** and the nicotinium cation. While the creatininium cation forms 1:1 and 2:1 complexes with ionophore **1**, the nicotinium cation interacts exclusively with the shallow and electronic rich aromatic cavity defined by the pyrrole rings of ionophore **1** in cone conformation.

As a way to overcome this problem, the development of a sensing array, measurements at different pHs and use of multivariate analysis has been successfully demonstrated. Regarding the array of sensors, during the last decade there has been significant improvements in the mass manufacturing and cost reduction of both, sensors and instrumentation. For this reason, addition of sensors should not represent any kind of problem. On the contrary, it is quite likely the path for the future development of more robust analytical tools. The major complication of the methodology proposed is without any doubt the measurement at different pH. While more work on this area will be required, recent progress in microfluidics and sample conditioning approaches in paper-based devices could be a way to automate the process and reduce all manual operations. Finally, the use of multivariate algorithms has been crucial to properly extract the information and estimate errors. It could be expected that through the addition of more channels of information, and through the use of more complex data analysis tools these methodologies could provide robust multianalyte monitoring tools.

Author contributions

(AC), (AFS), (PBl), (BG), (JR), (PBa) and **(FJA):** Conceptualization, methodology and investigation. **AC, AFS**: formal analysis. **PBl, BG, JR, PBa, FJA**: supervision. **AC, AFS**, **PBl:** writing-original draft. **PBl, BG, JR, PBa, FJA**: Writing - Review & Editing.

Declaration of competing interest

The authors declare that they have no known competing financial interests or personal relationships that could have appeared to influence the work reported in this paper.

Acknowledgments

AC would like to thank the support from an Erasmus fellowship. AC, PBl, JR and FJA would like to acknowledge the financial support from the Spanish ministry of Economy and Competitiveness (MICIN), the European Regional Development Fund (ERDF) and the agencia estatal de investigacion (AEI) (Project CTQ2016-77128-R and PID2019-106862RB-I00). AFS and PBa thank Gobierno de España MICIN/AEI/FEDER, UE (CTQ2017-84319-P, CEX2019-000925-S, and PID2020-114020 GB-I00), the CERCA Programme/Generalitat de Catalunya, and

AGAUR (2017 SGR 1123) for financial support.

Appendix A. Supplementary data

Supplementary data to this article can be found online at https://doi.org/10.1016/j.talanta.2022.123473.

References

[1] M. Baumgarten, T. Gehr, Chronic kidney disease: detection and evaluation, Am. Fam. Physician 84 (2011) 1138–1148.

[2] Team Healthy Aging, The top 10 most common chronic conditions in older adults, Natl. Counc. Aging (2021) (accessed October 19, 2021), https://www.ncoa.org/article/the-top-10-most-common-chronic-conditions-in-older-adults.

[3] J.R. Delanghe, M.M. Speeckaert, Creatinine determination according to Jaffe–what does it stand for? Clin. Kidney J. 4 (2011) 83–86, https://doi.org/10.1093/ndtplus/sfq211.

[4] P. Bühlmann, M. Hayakawa, T. Ohshiro, S. Amemiya, Y. Umezawa, Influence of natural, electrically neutral lipids on the potentiometric responses of cation-selective polymeric membrane electrodes, Anal. Chem. 73 (2001) 3199–3205, https://doi.org/10.1021/ac0015016.

[5] M.A.F. Elmosallamy, New potentiometric sensors for creatinine, Anal. Chim. Acta 564 (2006) 253–257, https://doi.org/10.1016/j.aca.2006.01.103.

[6] M.H. Gault, M.E. Seymour, W.E. Howell, Evaluation of i-STAT creatinine assay, Nephron 88 (2001) 178–182, https://doi.org/10.1159/000045982.

[7] T. Guinovart, D. Hernández-Alonso, L. Adriaenssens, P. Blondeau, M. Martínez-Belmonte, F.X. Rius, F.J. Andrade, P. Ballester, Recognition and sensing of creatinine, Angew. Chem. Int. Ed. 55 (2016) 2435–2440, https://doi.org/10.1002/anie.201510136.

[8] T. Guinovart, D. Hernández-Alonso, L. Adriaenssens, P. Blondeau, F.X. Rius, P. Ballester, F.J. Andrade, Characterization of a new ionophore-based ion-selective electrode for the potentiometric determination of creatinine in urine, Biosens. Bioelectron. 87 (2017) 587–592, https://doi.org/10.1016/j.bios.2016.08.025.

[9] J.L. Sessler, D.E. Gross, W.-S. Cho, V.M. Lynch, F.P. Schmidtchen, G.W. Bates, M. E. Light, P.A. Gale, Calix[4]pyrrole as a chloride anion receptor: solvent and countercation effects, J. Am. Chem. Soc. 128 (2006) 12281–12288, https://doi.org/10.1021/ja064012h.

[10] J. Chin, C. Walsdorff, B. Stranix, J. Oh, H.J. Chung, S.M. Park, K. Kim, A rational approach to selective recognition of NH(4)(+) over K(+), Angew. Chem., Int. Ed. Engl. 38 (1999) 2756–2759.

[11] J. Sabek, L. Adriaenssens, T. Guinovart, E.J. Parra, F.X. Rius, P. Ballester, P. Blondeau, Chloride-selective electrodes based on “two-wall” aryl-extended calix [4]Pyrroles: combining hydrogen bonds and anion-π interactions to achieve optimum performance, Chem. Eur J. 21 (2015) 448–454, https://doi.org/10.1002/chem.201403853.

[12] P. Bühlmann, L.D. Chen, Ion-selective electrodes with ionophore-doped sensing membranes, in: A.W. Steed, P. Gale (Eds.), Supramol. Chem. From Mol. to Nanomater., John Wiley & Sons, Ltd, 2012, pp. 2539–2579.

[13] V. V Egorov, V.A. Nazarov, E.B. Okaev, T.E. Pavlova, A new sulfate-selective electrode and its use in analysis, J. Anal. Chem. 61 (2006) 382–388, https://doi.org/10.1134/S1061934806040150.

[14] M. del Valle, Materials for electronic tongues: smart sensor combining different materials and chemometric tools, in: T.R.L. Cesar Paixão, S.M. Reddy (Eds.), Mater. Chem. Sens., Springer International Publishing, Cham, 2017, pp. 227–265, https://doi.org/10.1007/978-3-319-47835-7_9.

[15] M.N. Piña, B. Soberats, C. Rotger, P. Ballester, P.M. Deyà, A. Costa, Selective sensing of competitive anions by non-selective hosts: the case of sulfate and phosphate in water, New J. Chem. 32 (2008) 1919, https://doi.org/10.1039/b809454c.

[16] E. Bakker, E. Pretsch, P. Bühlmann, Selectivity of potentiometric ion sensors, Anal. Chem. 72 (2000) 1127–1133, https://doi.org/10.1021/ac991146n.

[17] U. Oesch, D. Ammann, W. Simon, Ion-selective membrane electrodes for clinical use, Clin. Chem. 32 (1986) 1448–1459.

[18] S.S.M. Hassan, E.M. Elnemma, Liquid membrane electrodes for the selective determination of nicotine in cigarette smoke, Analyst 114 (1989) 1033–1037, https://doi.org/10.1039/AN9891401033.

[19] A.E.-G.E. Amr, A.H. Kamel, A.A. Almehizia, A.Y.A. Sayed, E.A. Elsayed, H.S. M. Abd-Rabboh, Paper-based potentiometric sensors for nicotine determination in smokers’ sweat, ACS Omega 6 (2021) 11340–11347, https://doi.org/10.1021/acsomega.1c00301.

[20] C.E. Efstathiou, E.P. Diamandis, T.P. Hadjiioannou, Potentiometric determination of nicotine in tobacco products with a nicotine-sensitive liquid membrane electrode, Anal. Chim. Acta 127 (1981) 173–180, https://doi.org/10.1016/S0003-2670(01)83973-8.

[21] P. David, Composition and Concentrative Administration, NASA Contract. Rep, 1971, pp. 1–107. https://ntrs.nasa.gov/citations/19710023044.

[22] X. Xu, M.M. Iba, C.P. Weisel, Simultaneous and sensitive measurement of anabasine, nicotine, and nicotine metabolites in human urine by liquid chromatography–tandem mass spectrometry, Clin. Chem. 50 (2004) 2323–2330, https://doi.org/10.1373/clinchem.2004.038489.

[23] TURBOMOLE V7.0 2015, 2015. http://www.turbomole.com.

[24] J.P. Perdew, Density-functional approximation for the correlation energy of the inhomogeneous electron gas, Phys. Rev. B 33 (1986) 8822–8824, https://doi.org/10.1103/PhysRevB.33.8822.

[25] S. Grimme, J. Antony, S. Ehrlich, H. Krieg, A consistent and accurate ab initio parametrization of density functional dispersion correction (DFT-D) for the 94 elements H-Pu, J. Chem. Phys. 132 (2010) 154104, https://doi.org/10.1063/1.3382344.

[26] F. Weigend, R. Ahlrichs, Balanced basis sets of split valence, triple zeta valence and quadruple zeta valence quality for H to Rn: design and assessment of accuracy, Phys. Chem. Chem. Phys. 7 (2005) 3297–3305, https://doi.org/10.1039/B508541A.

[27] H. Parastar, D. Kirsanov, Analytical figures of merit for multisensor arrays, ACS Sens. 5 (2020) 580–587, https://doi.org/10.1021/acssensors.9b02531.